

High heat fluxes testing of tungsten materials with different microstructure under QSPA transient plasma impacts

V.A. Makhrai^{1,2}, I. E. Garkusha^{1,2}, S. S. Herashchenko^{1,2}, O.V. Byrka¹, N.N. Aksenov¹,
S.V. Malykhin³, S.V. Surovitskiy³, M. Wirtz⁴

¹ National Science Center Kharkov Institute of Physics and Technology, Institute of Plasma Physics, Kharkiv, Ukraine

² V.N. Karazin Kharkiv National University, Kharkiv, Ukraine

³ National Technical University 'Kharkiv Polytechnic Institute', Kharkiv, Ukraine

⁴ Forschungszentrum Jülich GmbH, Institut für Energie- und Klimaforschung, 52425 Jülich, Germany

Introduction

Tungsten is now considered the primary material for the armour of plasma-facing components in the divertor region of fusion devices like ITER and DEMO. The development of advanced tungsten grades requires thorough testing and qualification of material in extreme fusion relevant conditions, including both high heat and particle fluxes (H isotopes, He, and neutron) [1-3].

Accumulation and comparing data from a number of very different test facilities (electron, ion, and plasma) might be the basis for choosing the material with much better properties. For this reason, the main objective of this work is to study the features of macroscopic erosion of the pure tungsten irradiated by plasma streams in the powerful plasma accelerator QSPA Kh-50. That is considered to be an important direction of experimental research on the damage of different grades of tungsten as the major plasma facing material relevant to ITER and DEMO.

Experimental facility, samples, and diagnostics

Plasma-heat load tests of tungsten with energy density, pulse duration, and particle loads relevant to ITER transient events have been carried out in a QSPA Kh-50 quasi-stationary plasma accelerator [4, 5]. Samples of pure tungsten with the longitudinal (L) and transversal (T) grain orientation and in the recrystallized (R) state were used for the experiments [6]. Samples have sizes of $(12 \times 12 \times 5) \text{ mm}^3$. All specimens were polished to achieve a mirror-like surface. The samples were supplied by Plansee AG, prepared and delivered from Forschungszentrum Jülich.

The main parameters of the hydrogen plasma streams were as follows: ion impact energy of about 0.4 keV, maximum plasma pressure of 0.32 MPa, and stream diameter of 18 cm. The plasma pulse shape was approximately triangular, pulse duration of 0.25 ms. The surface

energy loads measured with a calorimeter were 0.1 MJ/m^2 (below the tungsten melting threshold (0.6 MJ/m^2)) and 0.75 MJ/m^2 (resulting in the melting of the tungsten surface) [4, 5].

Surface analysis of exposed samples was carried out with Scanning Electron Microscopy (SEM) JEOL JSM-6390. X-ray diffraction (XRD) has been used to study the structure, sub-structure, and stress state of targets. 9-29 scans were performed using monochromatic $\text{Cu-K}\alpha$ radiation [5, 7, 8]. The analysis of diffraction peaks intensity, profiles, width (B), and angular positions was applied to evaluate the texture and coherent scattering region size. Residual macro-stresses (σ) and the lattice parameter in the stress-free state (a_0) were determined using $a\text{-}\sin^2\psi$ -plots [5, 8] by the peaks (400) located in the precision area of angles (Fig. 1). The dashed vertical line showed the stress-free cross-section according to which a_0 was determined. If the lattice parameter in the stress-free state (a_0) is less than the corresponding reference value ($a_{\text{ref}}=0.3165 \text{ nm}$) then a lot of vacancies are present in the structure. If $a_0 > a_{\text{ref}}$ the surplus interstitial atoms are observed in the structure. It can be also attributed to alloying of tungsten by heavy elements.

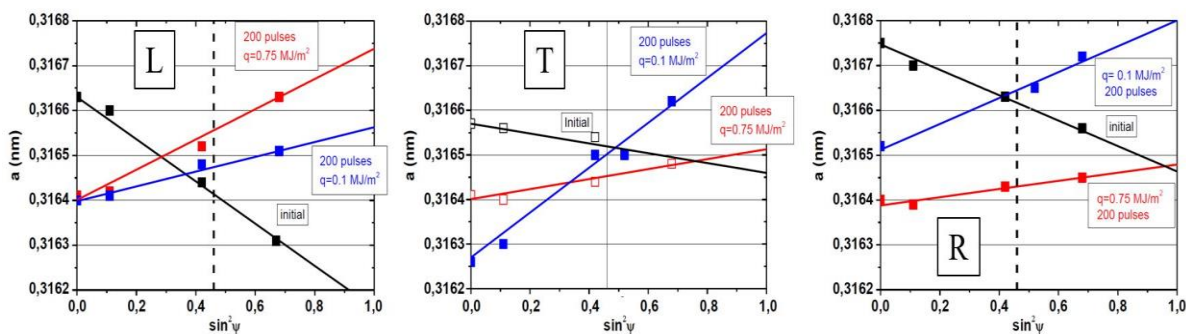


Fig. 1. $a\text{-}\sin^2\psi$ -plots for the L, T, and R samples of pure tungsten in an initial state (black line) as well as after irradiation by 200 plasma pulses of 0.1 MJ/m^2 (blue lines) and 0.75 MJ/m^2 (red lines).

Experimental results.

The samples were characterized following parameters in an initial state. Compressive stresses were registered for all samples with values of (108-409) MPa. Lattice spacing was below the reference value for the L sample (i.e., surplus vacancies were presented in the structure). Lattice spacing was near the reference value for the T sample. Lattice spacing was above the reference value for the R sample (i.e., surplus interstitial atoms were presented). SEM images of targets surfaces in the initial state as well as after plasma irradiation are presented in Fig. 2.-Fig. 4.

Plasma irradiation led to appearing of tensile stresses in all targets Fig. 1. Residual stresses grew with the increase of heat load. Heat load above the melting threshold led to the annealing of residual stresses in the re-solidified layer. Single vacancies were annealed in the surface

structure of the L sample. The lattice spacing did not change substantially in the T sample after plasma irradiation. Lattice spacing of the R sample decreased at irradiation with heat load above the melting threshold. Plasma irradiation with heat loads below the melting threshold resulted in surface modification of all samples (Fig. 3). Single cracks, as well as the porosity, were observed on exposed surfaces of all samples. The boundaries of grains became visible on the R target.

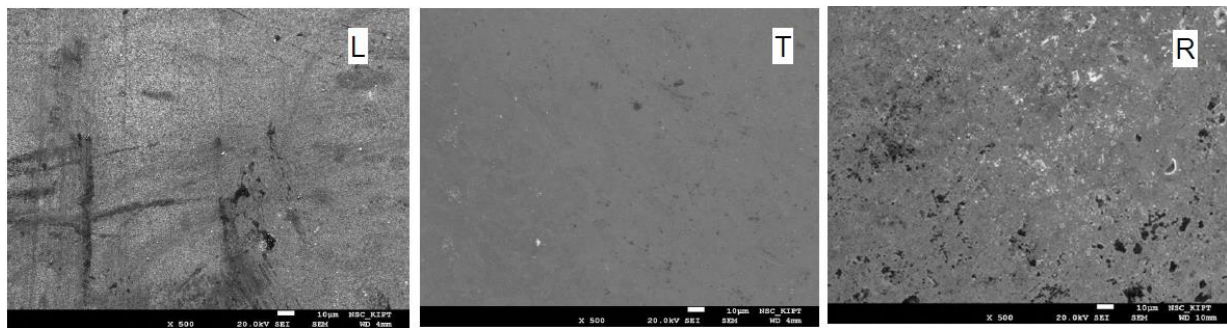


Fig. 2. SEM images of the L, T, and R samples in the initial state.

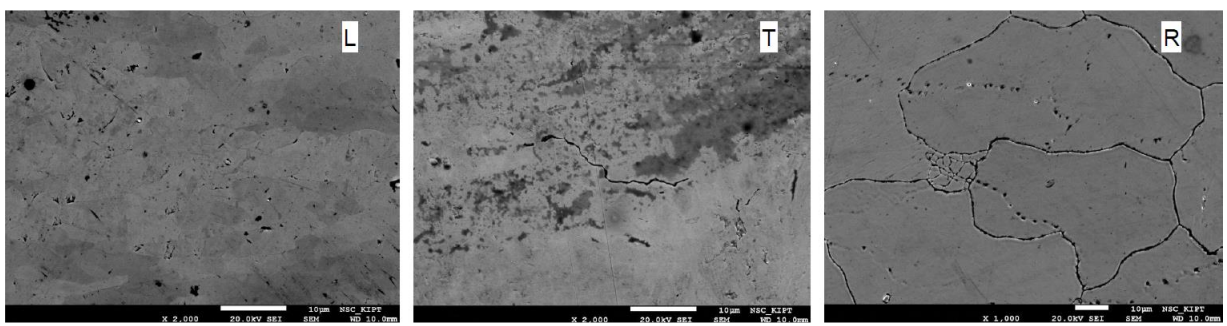


Fig.3 SEM images of the L, T, and R tungsten surfaces exposed to 200 plasma pulses of 0.1 MJ/m^2 each in the case of the initial surface temperature close to room temperature (RT).

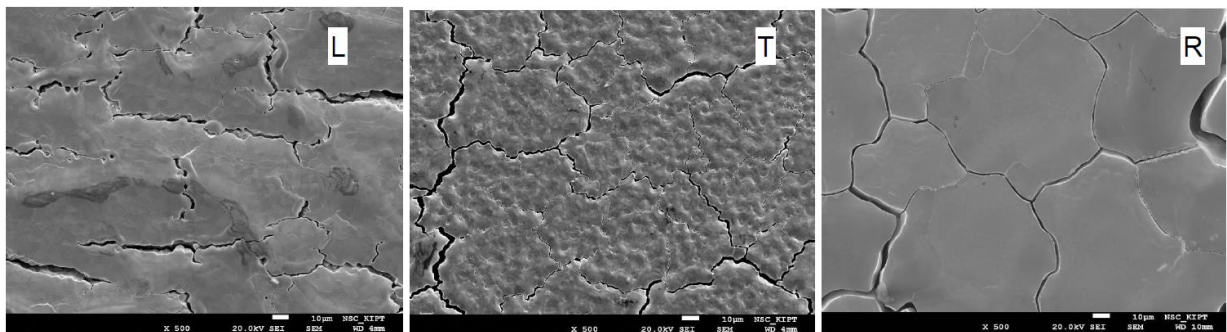


Fig.4 SEM images of the L, T, and R tungsten surfaces exposed to 200 plasma pulses of 0.75 MJ/m^2 each at the initial surface temperature of $T_{in} = 400 \text{ C}$.

Samples surfaces irradiated by plasma loads above the melting threshold were characterized by the formation of melted/re-solidified layer and networks of intergranular cracks. The width of such cracks reached up to several μm (Fig. 4). The corrugated structure was also formed on exposed surfaces as a result of repetitive plasma impacts. It should be noted, that the exposed

surface of the R sample showed the presence of fine cellular structure of the surface layer under heat load above the melting threshold. The typical cell size of 150...250 nm (Fig. 5)

Conclusions

Experimental characterization of pure tungsten with longitudinal (L), transversal (T) grain orientation, and in the recrystallized (R) state has been performed with a quasi-stationary plasma accelerator QSPA Kh-50. The heat loads on the surface were 0.1 MJ/m² (i.e., below the melting threshold) or 0.75 MJ/m² (i.e., between the melting- and evaporation thresholds). The plasma pulse duration amounted to about 0.25 ms.

All samples were characterized by compressive residual stresses with values of (108-409) MPa. Tensile stresses appeared as a result of plasma irradiation. A maximal value of 440 MPa was registered for the transversal samples under heat load below the melting threshold. Heat loads above the melting threshold led to fast annealing of residual stresses in the re-solidified layer of the transversal and the recrystallized samples.

Surface modification of the re-solidified layer was registered at heat loads above the melting threshold. Corrugated structures and networks of intergranular cracks with widths up to several μm also appeared. The fine cellular structure was observed in the surface layer of the recrystallized sample. The typical cell size of 150...250 nm.

Heat loads below the melting threshold (0.1 MJ/m²) did not lead to substantial surface damage.

Acknowledgments

This work has been carried out within the framework of the EUROfusion Consortium, funded by the European Union via the Euratom Research and Training Programme (Grant Agreement No 101052200 — EUROfusion). Views and opinions expressed are however those of the author(s) only and do not necessarily reflect those of the European Union or the European Commission. Neither the European Union nor the European Commission can be held responsible for them.” Work performed under EUROfusionWPMAT. This work has also been supported by National Academy Science of Ukraine project 22X-02-04/2022, II-2/24-2022

References

1. S. Brezinsek et al. // Nuclear Fusion. 2017, v. 57, 116041.
2. T. Hirai et al. // Nuclear Materials and Energy. 2016, v. 9, p. 616-622.
3. Q. Zhou et al. // Fusion Engineering and Design. 2020, v. 159, 111879.
4. V.A. Makhraj et al. // Physica Scripta. 2021, v. 96, 124043.
5. S.V. Malykhin et al // Nuclear Inst. and Meth. in Physics Research B. 2020, v. 481, p. 6-11
6. M. Wirtz et al. // Nuclear Materials and Energy. 2017, v. 12, p. 148-155.
7. M.A. Krivoglaz, X-Ray and Neutron Diffraction in Nonideal Crystals, 1996
8. V. A. Makhraj et. al., Phys. Scr. 2009, v. T138, 014060